# Nonparametric data segmentation in multivariate time series via joint characteristic functions

By E. T. MCGONIGLE

School of Mathematical Sciences, University of Southampton, University Road, Southampton SO17 1BJ, U.K. e.t.mcgonigle@soton.ac.uk

AND H. CHO

School of Mathematics, University of Bristol, Woodland Road, Bristol BS8 1UG, U.K. haeran.cho@bristol.ac.uk

#### SUMMARY

Modern time series data often exhibit complex dependence and structural changes that are not easily characterized by shifts in the mean or model parameters. We propose a non-parametric data segmentation methodology for multivariate time series. By considering joint characteristic functions between the time series and its lagged values, our proposed method is able to detect changepoints in the marginal distribution, but also those in possibly non-linear serial dependence, all without the need to prespecify the type of changes. We show the theoretical consistency of our method in estimating the total number and the locations of the changepoints, and demonstrate its good performance against a variety of changepoint scenarios. We further demonstrate its usefulness in applications to seismology and economic time series.

Some key words: Changepoint detection; Joint characteristic function; Moving sum; Multivariate time series; Nonparametric data.

## 1. Introduction

Changepoint analysis has been an active area of research for decades, dating back to Page (1954). Literature on changepoint detection continues to expand rapidly due to its prominence in numerous applications, including biology (Jewell et al., 2020), financial analysis (Lavielle & Teyssiere, 2007) and environmental sciences (Carr et al., 2017). Considerable efforts have been made for developing computationally and statistically efficient methods for data segmentation, also known as multiple changepoint detection, in the mean of univariate data under independence (Killick et al., 2012; Frick et al., 2014; Fryzlewicz, 2014) and permitting serial dependence (Tecuapetla-Gómez & Munk, 2017; Dette et al., 2020; Cho & Kirch, 2022; Cho & Fryzlewicz, 2023). There also exist methods for detecting changes in the covariance (Aue et al., 2009; Wang et al., 2021), parameters under linear regression

(Bai & Perron, 1998; Xu et al., 2024) or other models (Fryzlewicz & Subba Rao, 2014; Safikhani & Shojaie, 2022) in fixed and high dimensions. For an overview, see Truong et al. (2020) and Cho & Kirch (2024).

Any departure from distributional assumptions such as independence and Gaussianity tends to result in poor performance of changepoint algorithms. Furthermore, it may not be realistic to assume any knowledge of the type of changepoint that occurs, or to make parametric assumptions on the data-generating process, for time series that possess complex structures and are observed over a long period. Searching for changepoints in one property of the data (e.g., the mean), when the time series instead undergoes changes in another (e.g., the variance), may lead to misleading conclusions and inference on such data. Therefore, it is desirable to develop flexible, nonparametric changepoint detection techniques that are applicable to detect general changes in the underlying distribution of serially dependent data.

There are several strategies for the nonparametric changepoint detection problem, such as those based on the empirical cumulative distribution and density functions (Carlstein, 1988; Zou et al., 2014; Haynes et al., 2017; Madrid Padilla et al., 2021, 2022, 2023; Vanegas et al., 2022), kernel transforms of the data (Harchaoui et al., 2009; Celisse et al., 2018; Arlot et al., 2019; Li et al., 2019) or *U*-statistics measuring the 'energy'-based distance between different distributions (Matteson & James, 2014; Chakraborty & Zhang, 2021; Boniece et al., 2023). There also exist graph-based methods applicable to non-Euclidean data (Chen & Zhang, 2015; Chu & Chen, 2019). All these methods can only detect changes in the marginal distribution of the data and, apart from Madrid Padilla et al. (2023), assume serial independence. We also mention Cho & Fryzlewicz (2012), Preuß et al. (2015) and Korkas & Fryzlewicz (2017), who addressed the problem of detecting changes in the second-order structure, but their methods do not have power against changes in nonlinear dependence.

We propose a nonparametric moving sum procedure for detecting changes in the joint characteristic function, which we refer to as the NP-MOJO procedure, that detects multiple changes in serial, possibly nonlinear dependence as well as marginal distributions of a multivariate time series  $\{X_t\}_{t=1}^n$ . We adopt a moving sum procedure to scan the data for multiple changepoints. The moving sum methodology has successfully been applied to a variety of changepoint testing (Chu et al., 1995; Huskova & Slaby, 2001) and data segmentation problems (Eichinger & Kirch, 2018). Here, we combine it with a detector statistic carefully designed to detect changes in the complex dependence structure beyond those detectable from considering the marginal distribution only. Specifically, we utilize an energy-based distributional discrepancy that measures any change in the joint characteristic function of the time series at some lag  $\ell \geqslant 0$ , which allows for detecting changes in the joint distribution of  $(X_t, X_{t+\ell})$  beyond the changes in their linear dependence. To the best of our knowledge, the NP-MOJO procedure is the first nonparametric methodology that is able to detect changes in nonlinear serial dependence in multivariate time series.

We establish that the NP-MOJO procedure achieves consistency in estimating the number and locations of changepoints for a given lag, providing convergence rates for the changepoint location estimators, and propose a methodology that extends this desirable property of a single-lag NP-MOJO procedure to multiple lags. Combined with a dependent multiplier bootstrapping procedure, the NP-MOJO procedure and its multi-lag extension perform well across a wide range of changepoint scenarios in simulations and real data applications. Accompanying R software implementing the NP-MOJO procedure is available as the R package CptNonPar (McGonigle & Cho, 2023; R Development Core Team, 2025) on CRAN.

## 2. Model and measure of discrepancy

We observe a multivariate time series  $\{X_t\}_{t=1}^n$  of (finite) dimension p, where

$$X_{t} = \sum_{j=0}^{q} X_{t}^{(j)} \mathbb{I}\{\theta_{j} + 1 \leqslant t \leqslant \theta_{j+1}\}$$
(1)

with 
$$X_t = (X_{t1}, ..., X_{tp})^T$$
 and  $0 = \theta_0 < \theta_1 < \cdots < \theta_q < \theta_{q+1} = n$ .

For each sequence  $\{X_t^{(j)}: t \ge 1\}$ , j = 0, ..., q, there exists an  $\mathbb{R}^p$ -valued measurable function  $g^{(j)}(\cdot) = \{g_1^{(j)}(\cdot), ..., g_p^{(j)}(\cdot)\}^T$  such that  $X_t^{(j)} = g^{(j)}(\mathcal{F}_t)$  with  $\mathcal{F}_t = \sigma(\varepsilon_s: s \le t)$ , and independent and identically distributed random elements  $\varepsilon_t$ . We assume that  $g^{(j-1)} \neq g^{(j)}$  for all j = 1, ..., q, such that, under model (1), the time series undergoes q changepoints at locations  $\Theta = \{\theta_1, ..., \theta_q\}$ , with the notational convention that  $\theta_0 = 0$  and  $\theta_{q+1} = n$ . That is,  $\{X_t\}_{t=1}^n$  consists of q+1 stationary segments where the jth segment is represented in terms of a segment-dependent 'output'  $g^{(j)}(\mathcal{F}_t)$ , with the common 'input'  $\mathcal{F}_t$  shared across segments such that dependence across the segments is not ruled out. Each segment has a nonlinear Wold representation as defined by Wu (2005); this representation includes commonly adopted time series models including autoregressive moving average and generalized autoregressive conditional heteroscedastic (GARCH) processes.

Denote by  $\langle x, y \rangle = x^T y$  the inner product of two vectors x and y, and by i the imaginary unit with  $i^2 = -1$ . At some integer  $\ell$ , define the joint characteristic function of  $\{X_t^{(j)}\}_{t \in \mathbb{Z}}$  at lag  $\ell$  as

$$\phi_{\ell}^{(j)}(u,v) = \mathbb{E}\{\exp(\iota\langle u, X_1^{(j)}\rangle + \iota\langle v, X_{1+\ell}^{(j)}\rangle)\}, \qquad 0 \leqslant j \leqslant q.$$

We propose to measure the size of changes between adjacent segments under (1) using an energy-based distributional discrepancy given by

$$d_{\ell}^{(j)} = \int_{\mathbb{R}^p} \int_{\mathbb{R}^p} |\phi_{\ell}^{(j)}(u, v) - \phi_{\ell}^{(j-1)}(u, v)|^2 w(u, v) \, \mathrm{d}u \, \mathrm{d}v, \qquad 1 \leqslant j \leqslant q, \tag{2}$$

where w(u,v) is a positive weight function for which the above integral exists. For given lag  $\ell \geqslant 0$ , the quantity  $d_{\ell}^{(j)}$  measures the weighted  $L_2$  norm of the distance between the lag- $\ell$  joint characteristic functions of  $\{X_t^{(j-1)}\}_{t\in\mathbb{Z}}$  and  $\{X_t^{(j)}\}_{t\in\mathbb{Z}}$ . A discrepancy measure of this form is a natural choice for nonparametric data segmentation, since the following result holds.

LEMMA 1. For any 
$$\ell \geqslant 0$$
,  $d_{\ell}^{(j)} = 0$  if and only if  $(X_1^{(j)}, X_{1+\ell}^{(j)}) \stackrel{d}{=} (X_1^{(j-1)}, X_{1+\ell}^{(j-1)})$ .

Lemma 1 extends the observation made by Matteson & James (2014) about the correspondence between the characteristic function and marginal distribution. It shows that, by considering the joint characteristic functions  $\phi_{\ell}^{(j)}(u,v)$  at multiple lags  $\ell \geq 0$ , the discrepancy  $d_{\ell}^{(j)}$  is able to capture changes in the serial dependence as well as those in the marginal distribution of  $\{X_t\}_{t=1}^n$ .

The following lemma lists some choices of the weight function w(u, v) and the associated representation of  $d_{\ell}^{(j)}$  as the kernel-based discrepancy between  $Y_t^{(j)} = (X_t^{(j)}, X_{t+\ell}^{(j)})$  and  $Y_t^{(j-1)}$ , extending the observation made by Matteson & James (2014) for the setting where

a sequence of independent observations undergoes changes in the marginal distribution. Let ||x|| denote the Euclidean norm of a vector x, and define  $\tilde{Y}_t^{(j)} = (\tilde{X}_t^{(j)}, \tilde{X}_{t+\ell}^{(j)})$ , where  $\tilde{X}_t^{(j)} = g^{(j)}(\tilde{\mathcal{F}}_t)$  with  $\tilde{\mathcal{F}}_t = \sigma(\tilde{\varepsilon}_s \colon s \leqslant t)$  and  $\tilde{\varepsilon}_t$  is an independent copy of  $\varepsilon_t$ .

LEMMA 2.

(i) For any  $\beta > 0$ , suppose that  $d_{\ell}^{(j)}$  in (2) is obtained with respect to the weight function

$$w_1(u, v) = C_1(\beta, p)^{-2} \exp\left\{-\frac{1}{2\beta^2}(\|u\|^2 + \|v\|^2)\right\} \quad with \quad C_1(\beta, p) = (2\pi)^{p/2}\beta^p.$$

Then the function  $h_1: \mathbb{R}^{2p} \times \mathbb{R}^{2p} \to [0,1]$ , defined as  $h_1(x,y) = \exp(-\beta^2 ||x-y||^2/2)$  for  $x, y \in \mathbb{R}^{2p}$ , satisfies

$$d_{\ell}^{(j)} = \mathbb{E}\left\{h_1(Y_1^{(j)}, \tilde{Y}_1^{(j)})\right\} + \mathbb{E}\left\{h_1(Y_1^{(j-1)}, \tilde{Y}_1^{(j-1)})\right\} - 2\mathbb{E}\left\{h_1(\tilde{Y}_1^{(j)}, Y_1^{(j-1)})\right\}.$$

(ii) For any  $\delta > 0$ , suppose that  $d_{\ell}^{(j)}$  is obtained with

$$w_2(u,v) = C_2(\delta,p)^{-2} \prod_{s=1}^p u_s^2 v_s^2 \exp\left\{-\delta(u_s^2 + v_s^2)\right\}, \quad \text{where} \quad C_2(\delta,p) = \frac{\pi^{p/2}}{2^p \delta^{3p/2}}.$$

Then the function  $h_2: \mathbb{R}^{2p} \times \mathbb{R}^{2p} \to [-2e^{-2/3}, 1]$ , defined as

$$h_2(x,y) = \prod_{r=1}^{2p} \frac{\{2\delta - (x_r - y_r)^2\} \exp\{-(x_r - y_r)^2/4\delta\}}{2\delta}$$

for 
$$x = (x_1, ..., x_{2p})^T$$
 and  $y = (y_1, ..., y_{2p})^T$ , satisfies

$$d_{\ell}^{(j)} = \mathbb{E}\{h_2(Y_1^{(j)}, \tilde{Y}_1^{(j)})\} + \mathbb{E}\{h_2(Y_1^{(j-1)}, \tilde{Y}_1^{(j-1)})\} - 2\mathbb{E}\{h_2(\tilde{Y}_1^{(j)}, Y_1^{(j-1)})\}.$$

Lemma 2 is a special case of Bochner's theorem applied to the chosen weight functions; see, for example, §5.3 of Sejdinovic et al. (2013). The weight function  $w_1$  is commonly referred to as the Gaussian weight function. Both  $w_1$  and  $w_2$  are unit integrable and separable in their arguments, such that  $d_{\ell}^{(j)}$  is well defined due to the boundedeness of the characteristic function. We provide an alternative weight function in the Supplementary Material and also refer the reader to Fan et al. (2017) for other suitable choices.

Remark 1. From Lemma 2,  $d_\ell^{(j)}$  can be viewed as the squared maximum mean discrepancy on a suitably defined reproducing kernel Hilbert space with the associated kernel function; see Lemma 6 of Gretton et al. (2012) and § 2.6 of Celisse et al. (2018). We also note the literature on the (auto)distance correlation for measuring and testing dependence in multivariate (Székely et al., 2007) and time series (Zhou, 2012; Fokianos & Pitsillou, 2017; Davis et al., 2018) settings.

Remark 2. In model (1) (and in our theoretical results), dimension p of the time series is assumed fixed. We would expect practical performance to deteriorate with increasing dimension since we use an energy-based method. For example, when the time series undergoes a

change in both the mean and variance, the pre- and post-change segments of the time series can be separated into an 'inner layer' and 'outer layer' based on their pairwise Euclidean distances. However, as Chen & Friedman (2017, p. 399) noted, 'data points in the outer layer find themselves to be closer to points in the inner layer than other points in the outer layer', due to the curse of dimensionality. See, for example, Ramdas et al. (2015) or Chu & Chen (2019, § 2.2) for further discussion.

#### 3. Methodology

# 3.1. The NP-MOJO procedure

In this section we describe our proposed NP-MOJO procedure. The identities given in Lemma 2 allow for the efficient computation of the statistics approximating  $d_{\ell}^{(j)}$  and their weighted sums, which form the basis for the NP-MOJO procedure for detecting multiple changepoints from a multivariate time series  $\{X_t\}_{t=1}^n$  under model (1). Throughout, we present the procedure with a generic kernel h associated with some weight function w. We first introduce the NP-MOJO procedure for the problem of detecting changes in the joint distribution of  $Y_t = (X_t, X_{t+\ell})$  at a given lag  $\ell \geqslant 0$ , and extend it to the multi-lag problem in § 3.3 below.

For fixed bandwidth  $G \in \mathbb{N}$ , the NP-MOJO procedure scans the data using a detector statistic computed on neighbouring moving windows of length G, which approximates the discrepancy between the local joint characteristic functions of the corresponding windows measured analogously as in (2). Specifically, the detector statistic at location k is given by the two-sample V-statistic

$$T_{\ell}(G,k) = \frac{1}{(G-\ell)^2} \left\{ \sum_{s,t=k-G+1}^{k-\ell} h(Y_s, Y_t) + \sum_{s,t=k+1}^{k+G-\ell} h(Y_s, Y_t) - 2 \sum_{s=k-G+1}^{k-\ell} \sum_{t=k+1}^{k+G-\ell} h(Y_s, Y_t) \right\}$$

for k = G, ..., n - G, as an estimator of the local discrepancy measure

$$\mathcal{D}_{\ell}(G,k) = \sum_{i=0}^{q} \left( \frac{G - \ell - |k - \theta_j|}{G - \ell} \right)^2 d_{\ell}^{(j)} \mathbb{I}\{|k - \theta_j| \leqslant G - \ell\}.$$

At given k, the statistic  $T_{\ell}(G, k)$  measures the difference in the distribution of  $Y_t$  over the disjoint intervals of length  $G - \ell$  around k, and satisfies

$$\mathbb{E}\{T_{\ell}(G,k)\} = \mathcal{D}_{\ell}(G,k) + \mathcal{O}(G^{-1/2}). \tag{3}$$

We have  $\mathcal{D}_{\ell}(G,k)=0$  when the section of the data  $\{X_t, |t-k| \leq G-\ell\}$  does not undergo a change and, accordingly,  $T_{\ell}(G,k)$  is expected to be close to zero. On the other hand, if  $|k-\theta_j| < G-\ell$  then  $\mathcal{D}_{\ell}(G,k)$  increases and then decreases around  $\theta_j$  with a local maximum at  $k=\theta_j$ . The statistic  $T_{\ell}(G,k)$  is expected to behave similarly: in particular, at any changepoint location  $\theta_j$ , we have  $\mathbb{E}\{T_{\ell}(G,\theta_j)\}=d_{\ell}^{(j)}+\mathcal{O}(G^{-1/2})$  (see Lemma D.4 within the Supplementary Material for further information). We illustrate this using the following example.

Example 1. A univariate time series  $\{X_t\}_{t=1}^n$  of length n=1000 is generated as  $X_t=\mu_t+\varepsilon_t$ , where  $\mu_t=0.7\mathbb{I}\{t>\theta_1\}$  and  $\varepsilon_t=\varepsilon_t^{(1)}\mathbb{I}\{t<\theta_2\}+\varepsilon_t^{(2)}\mathbb{I}\{t\geqslant\theta_2\}$ , with  $\theta_1=300$  and

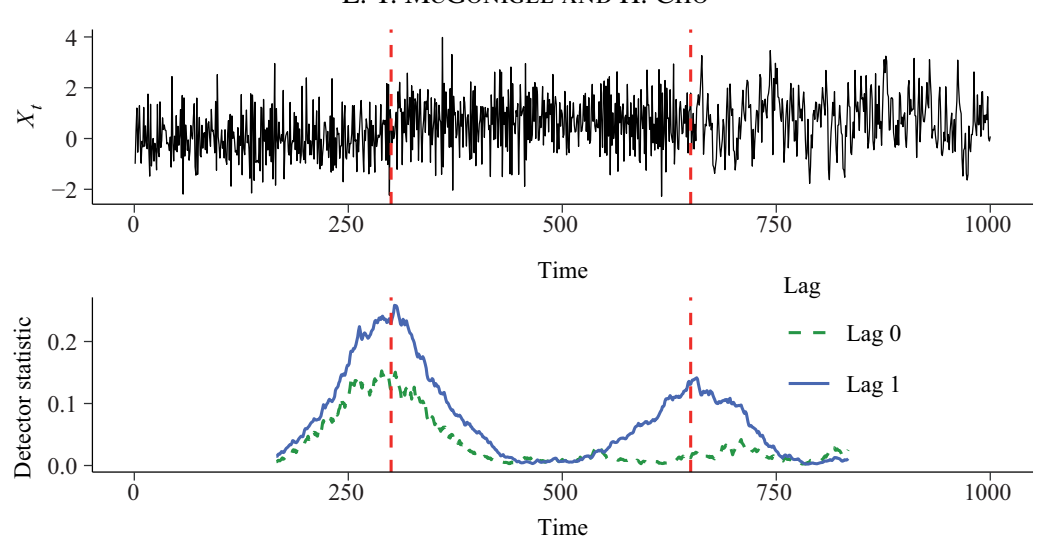


Fig. 1. Top: time series of length n=1000 with changepoints  $\theta_1=300$  and  $\theta_2=650$  (vertical dashed lines); see Example 1. Bottom: corresponding detector statistics  $T_{\ell}(G,k)$  computed at lags  $\ell=0$  (dashed) and  $\ell=1$  (solid).

 $\theta_2=650$ . Each  $\varepsilon_t^{(j)}$  is an autoregressive (AR) process of order 1, i.e.,  $\varepsilon_t^{(1)}=0.5\varepsilon_{t-1}^{(1)}+W_t$  and  $\varepsilon_t^{(2)}=-0.5\varepsilon_{t-1}^{(2)}+W_t$ , where  $\{W_t\}_{t\in\mathbb{Z}}$  is a white noise process with  $\mathrm{var}(W_t)=(1-0.5^2)^{1/2}$ . This choice leads to  $\mathrm{var}(X_t)=1$  for all t; see the top panel of Fig. 1 for a realization. Then, the mean shift at  $\theta_1$  is detectable at all lags, while the autocorrelation change at  $\theta_2$  is detectable at odd lags only, i.e.,  $d_\ell^{(2)}=0$  for even  $\ell\geqslant 0$ . The bottom panel of Fig. 1 plots  $T_\ell(G,k), G\leqslant k\leqslant n-G$ , computed using kernel  $h_2$  in Lemma 2(ii) with G=166. At lag  $\ell=0$ , the detector statistic forms a prominent peak around  $\theta_1$ , but it is flat around  $\theta_2$ ; at lag  $\ell=1$ , the statistic  $T_1(G,k)$  forms local maxima around both  $\theta_j, j=1,2$ .

Based on these observations, it is reasonable to detect and locate the changepoints in the joint distribution of  $(X_t, X_{t+\ell})$  as significant local maximizers of  $T_{\ell}(G, k)$ . We adopt the selection criterion, first considered by Eichinger & Kirch (2018) in the context of detecting mean shifts from univariate time series, for simultaneous estimation of multiple changepoints. For some fixed constant  $\eta \in (0, 1)$  and a threshold  $\zeta_{\ell}(n, G) > 0$ , we identify any local maximizer of  $T_{\ell}(G, k)$ , say  $\hat{\theta}$ , which satisfies

$$T_{\ell}(G,\hat{\theta}) > \zeta_{\ell}(n,G)$$
 and  $\hat{\theta} = \underset{k: |k-\hat{\theta}| \leq nG}{\arg \max} T_{\ell}(G,k).$  (4)

That is,  $\hat{\theta}$  is declared a changepoint if it is a local maximizer of  $T_{\ell}(G,k)$  over a sufficiently large interval of size  $\eta G$ , at which the threshold  $\zeta_{\ell}(n,G)$  is exceeded. We denote the set of such estimators fulfilling (4) by  $\hat{\Theta}_{\ell}$  with  $\hat{q}_{\ell} = |\hat{\Theta}_{\ell}|$ . The choice of  $\zeta_{\ell}(n,G)$  is discussed in § 3.4 below.

## 3.2. Theoretical properties

For some finite integer  $\ell \ge 0$ , we define the index set of changepoints detectable at lag  $\ell$  as  $\mathcal{I}_{\ell} = \{1 \le j \le q : d_{\ell}^{(j)} \ne 0\}$ , and denote its cardinality by  $q_{\ell} = |\mathcal{I}_{\ell}| \le q$ . Not all changepoints are detectable at all lags; see Example 1 where we have  $\mathcal{I}_0 = \{1\}$  and  $\mathcal{I}_1 = \{1, 2\}$ . In this section, we show that the estimated changepoints  $\hat{\Theta}_{\ell}$  produced by the single-lag NP-MOJO

procedure described in § 3.1 consistently estimates the total number  $q_{\ell}$  and the locations  $\{\theta_i, j \in \mathcal{I}_{\ell}\}$  of the changepoints detectable at lag  $\ell$ .

Writing  $g_{ti}(\cdot) = \sum_{j=0}^{q} g_i^{(j)}(\cdot) \mathbb{I}\{\theta_j + 1 \leq t \leq \theta_{j+1}\}$ , define  $X_{ti,\{t-s\}} = g_{ti}(\mathcal{F}_{t,\{t-s\}})$ , where  $F_{t,\{t-s\}} = \sigma(\dots, \varepsilon_{t-s-1}, \tilde{\varepsilon}_{t-s}, \varepsilon_{t-s+1}, \dots, \varepsilon_t)$  is a coupled version of  $\mathcal{F}_t$  with  $\varepsilon_{t-s}$  replaced by its independent copy  $\tilde{\varepsilon}_{t-s}$ . For a random variable Z and v > 0, let  $\|Z\|_v = \{\mathbb{E}(|Z|^v)\}^{1/v}$ . Analogously as in Xu et al. (2024), we define the elementwise functional dependence measure and its cumulative version as

$$\delta_{s,\nu,i} = \sup_{t \in \mathbb{Z}} \|X_{ti} - X_{ti,\{t-s\}}\|_{\nu} \quad \text{and} \quad \Delta_{m,\nu} = \max_{1 \leqslant i \leqslant p} \sum_{s=m}^{\infty} \delta_{s,\nu,i}, \quad m \in \mathbb{Z}.$$

Then, we make the following assumptions on the degree of serial dependence in  $\{X_t\}_{t=1}^n$ . Assumption 1. There exist some constants  $C_F$ ,  $C_X \in (0, \infty)$  and  $\gamma_1 \in (0, 2)$  such that

$$\sup_{m\geqslant 0}\exp(C_Fm^{\gamma_1})\Delta_{m,2}\leqslant C_X.$$

Assumption 2. The time series  $\{X_t\}_{t=1}^n$  is continuous and  $\beta$  mixing with  $\beta(m) \leqslant C_{\beta} m^{-\gamma_2}$  for some constants  $C_{\beta} \in (0, \infty)$  and  $\gamma_2 \geqslant 1$ , where

$$\beta(m) = \sup_{t \in \mathbb{Z}} \left( \sup \frac{1}{2} \sum_{r=1}^{R} \sum_{s=1}^{S} |\mathsf{pr}(A_r \cap B_s) - \mathsf{pr}(A_r) \mathsf{pr}(B_s)| \right).$$

Here, the inner supremum is taken over all pairs of finite partitions  $\{A_1, ..., A_R\}$  of  $\mathcal{F}_t = \sigma(\varepsilon_u, u \leq t)$  and  $\{B_1, ..., B_S\}$  of  $\sigma(\varepsilon_u, u \geq t + m)$ .

Assumptions 1 and 2 require the serial dependence in  $\{X_t\}_{t=1}^n$ , measured by  $\Delta_{m,2}$  and  $\beta(m)$ , to decay exponentially, and both are met by a range of linear and nonlinear processes (Mokkadem, 1988; Wu, 2005). Under Assumption 1,  $\|X_{it}\|_2 < \infty$  for all i and t. Assumption 1 is required for bounding  $T_\ell(G,k) - \mathbb{E}\{T_\ell(G,k)\}$  uniformly over k, while Assumption 2 is used for controlling the bias  $\mathbb{E}\{T_\ell(G,k)\} - \mathcal{D}_\ell(G,k)$  that is attributed to serial dependence. A condition similar to Assumption 2 is often found in the time series literature making use of distance correlations; see, e.g., Davis et al. (2018) and Yousuf & Feng (2022). Under the stronger assumption that  $\{X_t^{(j)}\}$  and  $\{X_t^{(j+1)}\}$  are independent, we can derive the analogous results to those presented in Theorems 1 and 3 below, under Assumption 2 only.

Assumption 3. The kernel function h is symmetric and bounded, and can be written as  $h(x,y) = h_0(x-y)$  for some function  $h_0 : \mathbb{R}^{2p} \to \mathbb{R}$  that is Lipschitz continuous with respect to  $\|\cdot\|$  with Lipschitz constant  $C_h \in (0,\infty)$ .

Assumption 3 on the kernel function h is met by  $h_1$  and  $h_2$  introduced in Lemma 2, with constants  $C_h$  bounded by  $\beta e^{-1/2}$  and  $2\sqrt{2}p^{3/2}\delta^{-1/2}$ , respectively.

Assumption 4.

- (i) As  $n \to \infty$ ,  $G^{-1}\log(n) \to 0$ , while  $\min_{0 \le j \le q} (\theta_{j+1} \theta_j) \ge 2G$ .
- (ii) We have  $\{G/\log(n)\}^{1/2} \min_{j \in \mathcal{I}_{\ell}} d_{\ell}^{(j)} \to \infty$ .

Recall that  $\mathcal{I}_{\ell}$  denotes the index set of detectable changepoints at lag  $\ell$ , i.e.,  $d_{\ell}^{(j)} > 0$  if and only if  $j \in \mathcal{I}_{\ell}$ . However, this definition of detectability is too weak to ensure that all  $\theta_j$ ,  $j \in \mathcal{I}_{\ell}$ , are detected by the NP-MOJO procedure with high probability at lag  $\ell$ , since we do not rule out the case of local changes where  $d_{\ell}^{(j)} \to 0$ . Consider Example 1: the change in the autocorrelations results in  $d_{\ell}^{(2)} > 0$  for all odd  $\ell$ , but the size of change is expected to decay exponentially fast as  $\ell$  increases. Assumption 4 allows for local changes provided that  $\{G/\log(n)\}^{1/2}d_{\ell}^{(j)}$  diverges sufficiently fast. Assumption 4(i), on the minimum spacing of changepoints, is commonly imposed in the literature on changepoint detection using moving window-based procedures. Assumption 4 does not rule out  $G/n \to 0$  and permits the number of changepoints q to increase in n. We discuss the selection of the bandwidth in §4 below.

Theorem 1. Suppose that Assumptions 1, 2, 3 and 4 hold, let  $\ell \geqslant 0$  be a finite integer and set the threshold as  $\zeta_{\ell}(n,G) = c_{\zeta} \{\log(n)/G\}^{1/2}$  for some constant  $c_{\zeta} > 0$ . Then, there exists  $c_0 > 0$ , depending only on  $C_F$ ,  $C_X$ ,  $\gamma_1$ ,  $C_{\beta}$ ,  $\gamma_2$  and p, such that, as  $n \to \infty$ ,

$$\operatorname{pr}\left(\hat{q}_{\ell} = q_{\ell}, \max_{j \in \mathcal{I}_{\ell}} \min_{\hat{\theta} \in \hat{\Theta}_{\ell}} d_{\ell}^{(j)} | \hat{\theta} - \theta_{j} | \leqslant c_{0} \{G \log(n)\}^{1/2}\right) \to 1.$$

Theorem 1 establishes that, for given  $\ell$ , the NP-MOJO procedure correctly estimates the total number and the locations of the changepoints detectable at lag  $\ell$  (including the nochange case where  $q_{\ell}=0$ ). In particular, by Assumption 4, the changepoint estimators satisfy

$$\min_{\hat{\theta} \in \hat{\Theta}_{\ell}} |\hat{\theta} - \theta_{j}| = O_{P}[(d_{\ell}^{(j)})^{-1} \{G \log(n)\}^{1/2}] = o_{P}\{\min(\theta_{j} - \theta_{j-1}, \theta_{j+1} - \theta_{j})\}$$

for all  $j \in \mathcal{I}_{\ell}$ , i.e., the changepoint estimators converge to the true changepoint locations in the rescaled time. Furthermore, the rate of estimation is inversely proportional to the size of change  $d_{\ell}^{(j)}$ , such that the changepoints associated with larger  $d_{\ell}^{(j)}$  are estimated with better accuracy. Also, making use of the energy-based distributional discrepancy, Matteson & James (2014) established the consistency of their proposed E-divisive method for detecting changes in the (marginal) distribution under independence. In addition to detection consistency, we further derive the rate of estimation for the NP-MOJO procedure that is applicable to detect changes in complex time series dependence besides those in marginal distribution, in broader situations permitting serial dependence.

Compared to the optimal rate of estimation known for some parametric changepoint problems, the rate reported in Theorem 1 is suboptimal due to the bias of order  $O(G^{-1/2})$  (see (3)) in U- and V-statistics in the presence of serial dependence. In the next theorem, we relax Assumptions 1 and 2 to serial independence, and derive a faster rate of estimation for detecting changepoints in the marginal distribution (namely,  $\theta_j$ ,  $j \in \mathcal{I}_0 = \{1, ..., q_0\}$ ) using the NP-MOJO procedure with lag  $\ell = 0$ .

THEOREM 2. Let Assumptions 3 and 4 hold, the latter with  $\ell = 0$ , and assume that  $\{X_t\}_{t=1}^n$  are independent over time, so that  $q_0 = q$ . Set the threshold as  $\zeta(n, G) = c_{\zeta} \{\log(n)/G\}^{1/2}$  for

some constant  $c_7 > 0$ . Then, there exists  $c_0 > 0$ , depending on p, such that, as  $n \to \infty$ ,

$$\operatorname{pr}\left(\hat{q}=q, \max_{1\leqslant j\leqslant q} \min_{\hat{\theta}\in\hat{\Theta}_0} (d_0^{(j)})^2 |\hat{\theta}-\theta_j|\leqslant c_0\log(n)\right) \to 1.$$

# 3.3. Multi-lag extension of the NP-MOJO procedure

In this section, we address the problem of combining the results of the NP-MOJO procedure when it is applied with multiple lags. Let  $\mathcal{L} \subset \mathbb{N}_0 = \{0, 1, ...\}$  denote a (finite) set of nonnegative integers. Recall that, given  $\ell \in \mathcal{L}$ , the NP-MOJO procedure returns a set of changepoint estimators  $\hat{\Theta}_{\ell}$ . Denote the union of changepoint estimators over all lags  $\mathcal{L}$  by  $\tilde{\Theta} = \bigcup_{\ell \in \mathcal{L}} \hat{\Theta}_{\ell} = {\{\tilde{\theta}_j, 1 \leq j \leq Q \colon \tilde{\theta}_1 < \dots < \tilde{\theta}_Q\}}, \text{ and denote by } \mathbb{T}(\tilde{\theta}) = \max_{\ell \in \mathcal{L}} T_{\ell}(G, \tilde{\theta})$ the maximum detector statistic at  $\tilde{\theta}$  across all  $\tilde{\ell} \in \mathcal{L}$ . We propose to find a set of the final changepoint estimators  $\hat{\Theta} \subset \tilde{\Theta}$  by taking the following steps; we refer to this procedure as the multi-lag NP-MOJO procedure.

Step 0. Set  $\hat{\Theta} = \emptyset$  and select a constant  $c \in (0, 2]$ .

Step 1. Set  $\tilde{\Theta}_1 = \tilde{\Theta}$  and m = 1. Iterate steps 2–4 below for m = 1, 2, ..., while  $\tilde{\Theta}_m \neq \emptyset$ .

Step 2. Let  $\tilde{\theta}_m = \min \; \tilde{\Theta}_m \text{ and identify } \mathcal{C}_m = \{\tilde{\theta} \in \tilde{\Theta}_m : \tilde{\theta} - \tilde{\theta}_m < cG\}.$ Step 3. Identify  $\hat{\theta}_m = \arg \max_{\tilde{\theta} \in \mathcal{C}_m} \mathbb{T}(\tilde{\theta})$ ; if there is a tie, we arbitrarily break it.

Step 4. Add  $\hat{\theta}_m$  to  $\hat{\Theta}$  and update  $m \leftarrow m+1$  and  $\tilde{\Theta}_m = \tilde{\Theta}_{m-1} \setminus \mathcal{C}_{m-1}$ .

At iteration m of the multi-lag NP-MOJO procedure, Step 2 identifies the minimal element from the current set of candidate changepoint estimators  $\tilde{\Theta}_m$ , and a cluster of estimators  $C_m$  whose elements are expected to detect the identical changepoints from multiple lags. Then, Step 3 finds an estimator  $\hat{\theta} \in \mathcal{C}_m$ , which is associated with the largest detector statistic at some lag, and it is added to the set of final estimators. This choice is motivated by Theorem 1, which shows that each  $\theta_i$  is estimated with better accuracy at the lag associated with the largest change in the lagged dependence (measured by  $d_{\ell}^{(j)}$ ). Iterating these steps until all the elements of  $\tilde{\Theta}$  are either added to  $\hat{\Theta}$  or discarded, we obtain the set of final changepoint estimators.

We define a subset of  $\mathcal{L}$  containing the lags at which the *j*th changepoint is detectable as  $\mathcal{L}^{(j)} = \{\ell \in \mathcal{L} : d_{\ell}^{(j)} \neq 0\}$ . Revisiting Example 1, when we set  $\mathcal{L} = \{0, 1\}$ , it follows that  $\mathcal{L}^{(1)} = \{0, 1\}$  $\{0,1\}$  and  $\mathcal{L}^{(2)}=\{1\}$ . To establish the consistency of the multi-lag NP-MOJO procedure, we formally assume that all changepoints are detectable at some lag  $\ell \in \mathcal{L}$ .

Assumption 5. For  $\mathcal{L} \subset \mathbb{N}_0$  with  $L = |\mathcal{L}| < \infty$ , we have  $\bigcup_{\ell \in \mathcal{L}} \mathcal{I}_{\ell} = \{1, ..., q\}$ . Equivalently,  $\mathcal{L}^{(j)} \neq \emptyset$  for all j = 1, ..., q.

Under Assumptions 1–5, consistency of the multi-lag NP-MOJO procedure is largely a consequence of Theorem 1. Assumption 4(ii) requires that at any lag  $\ell \in \mathcal{L}$  and a given changepoint  $\theta_j$ , we have either  $j \in \mathcal{I}_{\ell}$  with  $d_{\ell}^{(j)}$  large enough (in the sense that  $\{G/\log(n)\}^{1/2}d_{\ell}^{(j)} \to \infty$ ), or  $j \notin \mathcal{I}_{\ell}$  such that  $d_{\ell}^{(j)} = 0$ . Such a dyadic classification of the changepoints rules out the possibility that, for some j, we have  $d_{\ell}^{(j)} > 0$ , but  $d_{\ell}^{(j)} = O\{\{\log(n)/G\}^{1/2}\}$ , in which case  $\theta_i$  may escape detection by the NP-MOJO procedure at lag  $\ell$ . We thus consider the following alternative.

Assumption 6.

- (i) As  $n \to \infty$ ,  $G^{-1} \log(n) \to 0$ , while  $\min_{0 \le i \le q} (\theta_{i+1} \theta_i) \ge 4G$ .
- (ii) We have  $\{G/\log(n)\}^{1/2} \min_{1 \le j \le q} \max_{\ell \in \mathcal{L}^{(j)}} d_{\ell}^{(j)} \to \infty$ .

Compared to Assumption 4, Assumption 6 requires that the changepoints are further apart from one another relative to G by the multiplicative factor of 2. At the same time, the latter only requires that, for each j=1,...,q, there exists at least one lag  $\ell\in\mathcal{L}$  at which  $d_{\ell}^{(j)}$  is large enough to guarantee the detection of  $\theta_j$  by the NP-MOJO procedure with large probability. Theorem 3 below establishes the consistency of the multi-lag NP-MOJO procedure under either Assumption 4 or 6.

Theorem 3. Suppose that Assumptions 1–3 and 5 hold, and at each  $\ell \in \mathcal{L}$  we set  $\zeta_{\ell}(n,G) = c_{\zeta,\ell} \{\log(n)/G\}^{1/2}$  with some constants  $c_{\zeta,\ell} > 0$ . Let  $\hat{\Theta} = \{\hat{\theta}_j, 1 \leq j \leq \hat{q} : \hat{\theta}_1 < \cdots < \hat{\theta}_{\hat{q}}\}$  denote the set of estimators returned by the multi-lag NP-MOJO procedure with tuning parameter c.

(i) If Assumption 4 holds for all  $\ell \in \mathcal{L}$  and  $c = 2\eta$  with  $\eta \in (0, 1/2]$  then, with  $c_0$  as in Theorem 1, depending only on  $C_F$ ,  $C_X$ ,  $\gamma_1$ ,  $C_\beta$ ,  $\gamma_2$  and p,

$$\operatorname{pr}\left(\hat{q}=q, \max_{1\leqslant j\leqslant q}\max_{\ell\in\mathcal{L}^{(j)}}d_{\ell}^{(j)}|\hat{\theta}_{j}-\theta_{j}|\leqslant c_{0}\{G\log(n)\}^{1/2}\right)\to 1 \quad \text{as } n\to\infty.$$

(ii) If Assumption 6 holds and c = 2 then the conclusion of part (i) holds.

Under Assumption 6(ii), which is weaker than Assumption 4(ii), we may encounter a situation where  $\{G/\log(n)\}^{1/2}d_\ell^{(j)}=O(1)$ , while  $d_\ell^{(j)}>0$  at some lag  $\ell\in\mathcal{L}$ . Then, we cannot guarantee that such  $\theta_j$  is detected by the NP-MOJO procedure at lag  $\ell$  and, even so, we can only show that its estimator  $\tilde{\theta}\in\tilde{\Theta}_\ell$  satisfies  $|\tilde{\theta}-\theta_j|=O(G)$ . This requires setting the tuning parameter c maximally for the clustering in Step 2 of the multi-lag NP-MOJO procedure; see Theorem 3(ii). At the same time, there exists a lag well suited for the localization of each changepoint and Step 3 identifies an estimator detected at such a lag, and the final estimator inherits the rate of estimation attained at the favourable lag.

# 3.4. Threshold selection via dependent wild bootstrap

Theorem 1 gives the choice of the threshold  $\zeta_{\ell}(n,G) = c_{\zeta} \{\log(n)/G\}^{1/2}$  that guarantees the consistency of the NP-MOJO procedure in multiple changepoint estimation. The choice of  $c_{\zeta}$  influences the finite sample performance of the NP-MOJO procedure, but it depends on many unknown quantities involved in specifying the degree of serial dependence in  $\{X_t\}_{t=1}^n$  (see Assumptions 1 and 2), which makes the theoretical choice of little practical use. Resampling is popularly adopted for the calibration of changepoint detection methods, including threshold selection. However, due to the presence of serial dependence, permutation-based approaches such as that adopted by Matteson & James (2014) or sample splitting adopted by Madrid Padilla et al. (2021) are inappropriate.

We propose to adopt the dependent wild bootstrap procedure proposed by Leucht & Neumann (2013), in order to approximate the quantiles of  $\max_{G \leqslant k \leqslant n-G} T_\ell(G,k)$  in the absence of any changepoint, from which we select  $\zeta_\ell(n,G)$ . Let  $\{W_t^{[r]}\}_{t=1}^{n-G}$  denote a bootstrap sequence generated as a Gaussian AR(1) process with  $\operatorname{var}(W_t^{[r]}) = 1$  and the AR coefficient  $\exp(-1/b_n)$ , where the sequence  $\{b_n\}$  is chosen such that  $b_n = o(n)$  and  $\lim_{n \to \infty} b_n = \infty$ .

We construct bootstrap replicates using  $\{W_t^{[r]}\}_{t=1}^{n-G}$  as  $T_\ell^{[r]} = \max_{G \leq k \leq n-G} T_\ell^{[r]}(G,k)$ , where

$$T_{\ell}^{[r]}(G,k) = \frac{1}{(G-\ell)^2} \left\{ \sum_{s,t=k-G+1}^{k-\ell} \bar{W}_{s,k}^{[r]} \bar{W}_{t,k}^{[r]} h(Y_s, Y_t) + \sum_{s,t=k+1}^{k+G-\ell} \bar{W}_{s-G,k}^{[r]} \bar{W}_{t-G,k}^{[r]} h(Y_s, Y_t) \right.$$
$$\left. - 2 \sum_{s=k-G+1}^{k-\ell} \sum_{t=k+1}^{k+G-\ell} \bar{W}_{s,k}^{[r]} \bar{W}_{t-G,k}^{[r]} h(Y_s, Y_t) \right\}$$

with  $\bar{W}_{t,k}^{[r]} = W_t^{[r]} - (G - \ell)^{-1} \sum_{u=k-G+1}^{k-\ell} W_u^{[r]}$ . Independently generating  $\{W_t^{[r]}\}_{t=1}^{n-G}$  for  $r=1,\ldots,R$  (R denoting the number of bootstrap replications), we store  $T_\ell^{[r]}$  and select the threshold as  $\zeta_\ell(n,G) = q_{1-\alpha}(\{T_\ell^{[r]}\}_{r=1}^R)$ , the  $(1-\alpha)$  quantile of  $\{T_\ell^{[r]}\}_{r=1}^R$  for the chosen level  $\alpha \in (0,1]$ . Additionally, we can compute the importance score for each  $\hat{\theta} \in \hat{\Theta}_\ell$  as

$$s(\hat{\theta}) = \frac{|\{1 \leqslant r \leqslant R \colon T_{\ell}(G, \hat{\theta}) \geqslant T_{\ell, r}^{[r]}\}|}{R}.$$

Taking a value between 0 and 1, the larger  $s(\hat{\theta})$  is, the more likely that there exists a change-point close to  $\hat{\theta}$  empirically. The bootstrap procedure generalizes to the multi-lag NP-MOJO procedure straightforwardly. In practice, we observe that setting  $\hat{\theta}_j = \arg\max_{\tilde{\theta} \in \mathcal{C}_j} s(\tilde{\theta})$  (with some misuse of the notation,  $s(\cdot)$  is computed at the relevant lag for each  $\tilde{\theta}$ ) works well in Step 3 of the multi-lag NP-MOJO procedure. This is attributed to the fact that this score inherently takes into account the varying scale of the detector statistics at multiple lags and 'standardizes' the importance of each estimator. In all numerical experiments, our implementation of the multi-lag NP-MOJO procedure is based on this choice of  $\hat{\theta}_j$ . We provide the algorithmic descriptions of the NP-MOJO procedure and its multi-lag extension in Algorithms 1 and 2 within the Supplementary Material.

#### 4. IMPLEMENTATION OF THE NP-MOJO PROCEDURE

## 4.1. Computational complexity

Owing to the moving sum-based approach, the cost of sequentially computing  $T_{\ell}(G,k)$  from  $T_{\ell}(G,k-1)$  is O(G), giving the overall cost of computing  $T_{\ell}(G,k)$ ,  $G \le k \le n-G$ , as O(nG). Exact details of the sequential update are given in the Supplementary Material. The bootstrap procedure described in § 3.4 is performed once per lag for simultaneously detecting multiple changepoints, in contrast with the E-divisive method (Matteson & James, 2014) that requires the permutation-based testing to be performed for detecting each changepoint. With R bootstrap replications, the total computational cost is  $O(|\mathcal{L}|RnG)$  for the multi-lag NP-MOJO procedure using the set of lags  $\mathcal{L}$  and bootstrapping, as opposed to  $O(Rqn^2)$  for the E-divisive method. Furthermore, the bootstrap procedure can be parallelized in a straightforward manner, which we include as an option in the implementation of the method.

We ran simulations to compare the computational speed of the competing nonparametric methods: E-divisive (Matteson & James, 2014), NWBS (Madrid Padilla et al., 2021), KCPA (Celisse et al., 2018; Arlot et al., 2019) and cpt.np (Haynes et al., 2017). We simulate realizations under the change in mean model (B.1) in the Supplementary Material,

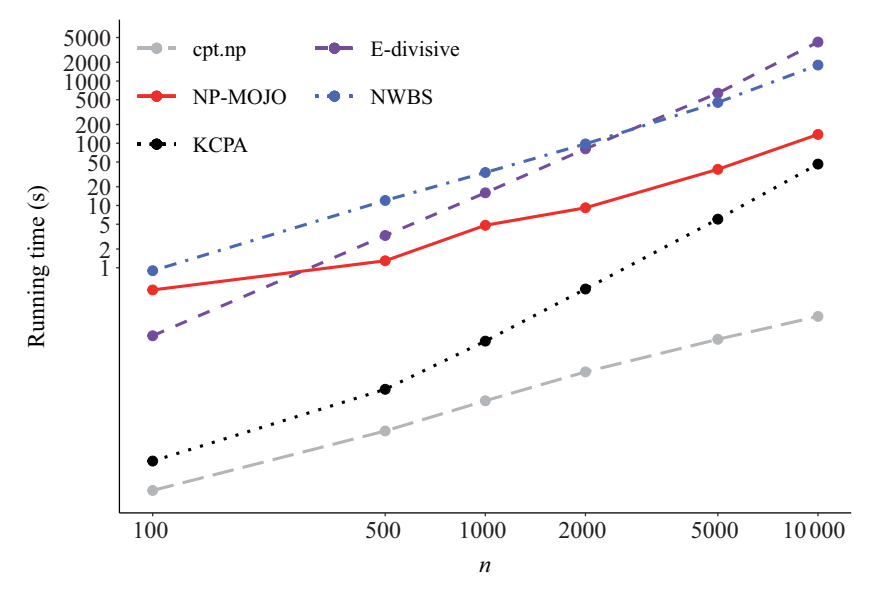


Fig. 2. Running time comparisons between the competing nonparametric methods.

Both axes are on the log scale.

with increasing values of sample size n and the number of equispaced changepoints q  $((n,q) \in \{(100,1),(500,2),(1000,3),(2000,5),(5000,10),(10000,20)\})$ . We use the same settings for each method as in the main simulation study, using the parallelized version of the multi-lag NP-MOJO procedure when  $n \ge 2000$ , and compute the average run time over 100 realizations. The results are displayed in Fig. 2. The fastest method by far is cpt.np, followed by KCPA and NP-MOJO. The E-divisive and NWBS methods are noticeably slower than the other methods. In particular, when  $n = 10\,000$ , the average running time is 0.17 s for cpt.np, 46.26 s for the KCPA method, 2.31 min for the NP-MOJO method, 30.06 min for the NWBS method and 70.37 min for the E-divisive method. Also, we observe that the KCPA method's running time increases at a faster rate than the NP-MOJO method's, and may exceed the running time of the NP-MOJO method for larger values of n.

## 4.2. Kernel function

As with any kernel-based approach, the NP-MOJO procedure's performance will vary with the choice of kernel, and a kernel that works well for one type of changepoint may not be the best for another type of changepoint. Based on empirical performance and versatility to a wide range of changepoint scenarios we recommend the use of the kernel function  $h_2$  in Lemma 2(ii). The parameter  $\delta$  is set using the 'median trick', a common heuristic used in kernel-based methods (Li et al., 2019). Specifically, we set  $\delta$  to be half the median of all  $||Y_s - Y_t||^2$  involved in the calculation of  $T_\ell(G, k)$ . For p-variate independent and identically distributed Gaussian data with common variance  $\sigma^2$ , this corresponds to  $\delta \approx \sigma p$  as dimension p increases (Ramdas et al., 2015). As with kernel  $h_2$ , the median trick can also be used when setting  $\beta$  if kernel  $h_1$  is used.

# 4.3. Bandwidth

Because of the nonparametric nature of the NP-MOJO procedure, it is advised to use a larger bandwidth than that shown to work well for the moving sum procedure for univariate mean change detection (Eichinger & Kirch, 2018). In our simulation studies and data applications, we set  $G = \lfloor n/6 \rfloor$ . It is often found that using multiple bandwidths

and merging the results improves the adaptivity of moving window-based procedures, such as the 'bottom-up' merging proposed by Messer et al. (2014) or the localized pruning of Cho & Kirch (2022). We empirically explore the multiscale extension of the multi-lag NP-MOJO procedure with bottom-up merging; see the Supplementary Material for details of its implementation and for a proof of the concept numerical study involving multiscale changepoint scenarios. We leave a theoretical investigation into the multiscale extension of the NP-MOJO procedure for future research.

# 4.4. Parameters for changepoint estimation

We set  $\eta = 0.4$  in (4) following the recommendation by Meier et al. (2021). For the multilag NP-MOJO procedure, we set c = 1 for clustering the estimators from multiple lags, a choice that lies between those recommended in Theorem 3(i) and (ii), since we do not know whether Assumption 4 or 6 holds in practice. In the Supplementary Material we demonstrate that, within a reasonable range, the NP-MOJO procedure is insensitive to the choices of  $\eta$  and c. To further guard against spurious estimators, we only accept those  $\hat{\theta}$  that lie in intervals of length greater than  $\lfloor 0.02G \rfloor$  where the corresponding  $T_{\ell}(G, k)$  exceeds  $\zeta_{\ell}(n, G)$ .

## 4.5. Parameters for the bootstrap procedure

The choice of  $b_n$  sets the level of dependence in the multiplier bootstrap sequences. Leucht & Neumann (2013) showed that a necessary condition is that  $\lim_{n\to\infty} (b_n^{-1} + b_n n^{-1}) = 0$ , giving a large freedom for the choice of  $b_n$ . We recommend  $b_n = 1.5n^{1/3}$ , which works well, in practice. In the Supplementary Material we demonstrate that, within a reasonable range, the NP-MOJO procedure is insensitive to the choice of  $b_n$ . As for  $\alpha$ , its choice amounts to setting the level of significance in statistical testing. This provides a more systematic alternative to the problem of model selection in multiple changepoint detection compared to others, such as those requiring the selection of a threshold that is known up to a rate (or a range of rates; see, e.g., Madrid Padilla et al., 2023), or constants involved in the penalty of a penalized cost function (Arlot et al., 2019). In all numerical experiments, we use  $\alpha = 0.1$  with R = 499 bootstrap replications.

# 4.6. Set of lags L

The flexibility of the NP-MOJO procedure in its ability to detect changes in dependence comes at the price of having to select the set of lags  $\mathcal{L}$ . The choice of  $\mathcal{L}$  depends on the practitioner's interest and domain knowledge, a problem commonly faced by general-purpose changepoint detection methods, such as the choice of the quantile level in Vanegas et al. (2022), the parameter of interest in Zhao et al. (2022) and the estimating equation in Kirch & Reckruehm (2024). For example, for monthly data, using  $\mathcal{L} = \{0, 3, 12\}$  allows for detecting changes in the quarterly and yearly seasonality. Even when the interest lies in detecting changes in the marginal distribution only, it helps to jointly consider multiple lags, since any marginal distributional change is likely to result in changes in the joint distribution of  $(X_t, X_{t+\ell})$ . As we consider time series that exhibit short-range dependence, we would expect that the NP-MOJO procedure will not have detection power at large lags. In simulations, we use  $\mathcal{L} = \{0, 1, 2\}$ , which works well not only for detecting changes in the mean and the second-order structure, but also for detecting changes in (nonlinear) serial dependence and higher-order characteristics. For a practical approach to lag selection, see the Supplementary Material, where we propose a semi-automatic method for choosing the set of lags  $\mathcal{L}$ given some initial set  $\hat{\mathcal{L}}$ .

## 5. SIMULATION STUDY

We conduct extensive simulation studies with varying changepoint scenarios (30 scenarios where  $q \ge 1$ , 7 with q = 0), sample sizes  $(n \in \{500, 1000, 2000, 10000\})$  and dimensions  $p \in \{1, 2, 5, 10\}$ , and consider both evenly spaced and multiscale changepoint settings. We provide complete descriptions of the simulation studies in the Supplementary Material where, for comparison, we consider, not only nonparametric, but also parametric data segmentation procedures well suited to detect the types of changes in consideration, which include changes in the mean, second-order and higher-order moments and nonlinear serial dependence. Owing to space constraints, here we focus on a selection of the results in the evenly spaced setting with n = 1000, comparing both single-lag and multi-lag NP-MOJO (denoted NP-MOJO- $\ell$  and NP-MOJO- $\mathcal{L}$ , respectively) procedures, with the nonparametric competitors: E-divisive (Matteson & James, 2014), NWBS (Madrid Padilla et al., 2021), KCPA (Celisse et al., 2018; Arlot et al., 2019) and cpt.np (Haynes et al., 2017). The E-divisive and KCPA methods are applicable to multivariate data segmentation, whilst the NWBS and cpt.np methods are not. The scenarios are

- (B5)  $X_t = \sum_{j=0}^{3} \Sigma_j^{1/2} \mathbb{I}\{\theta_j + 1 \leq t \leq \theta_{j+1}\} \cdot \varepsilon_t$ , where  $\varepsilon_t = (\varepsilon_{1t}, \varepsilon_{2t})^{\mathrm{T}}$  with  $\varepsilon_{it} \stackrel{\text{i.i.d.}}{\sim} t_5$ ,  $(\theta_1, \theta_2, \theta_3) = (250, 500, 750)$ ,  $\Sigma_0 = \Sigma_2 = \begin{pmatrix} 1 & 0 \\ 0 & 1 \end{pmatrix}$  and  $\Sigma_1 = \Sigma_3 = \begin{pmatrix} 1 & 0.9 \\ 0.9 & 1 \end{pmatrix}$ ;
- (C1)  $X_t = X_t^{(j)} = a_j X_{t-1}^{(j)} + \varepsilon_t \text{ for } \theta_j + 1 \le t \le \theta_{j+1}, \text{ where } q = 2, (\theta_1, \theta_2) = (333, 667) \text{ and } (a_0, a_1, a_2) = (-0.8, 0.8, -0.8);$ (C3)  $X_t = X_t^{(j)} = \sigma_t^{(j)} \varepsilon_t \text{ with } (\sigma_t^{(j)})^2 = \omega_j + \alpha_j (X_{t-1}^{(j)})^2 + \beta_j (\sigma_{t-1}^{(j)})^2 \text{ for } \theta_j + 1 \le t \le \theta_{j+1}, \text{ where } q = 1, \theta_1 = 500, (\omega_0, \alpha_0, \beta_0) = (0.01, 0.7, 0.2) \text{ and } (\omega_1, \alpha_1, \beta_1) = (0.01, 0.2, 0.7);$
- (D3)  $X_t = 0.4X_{t-1} + \varepsilon_t$  where  $\varepsilon_t \stackrel{\text{i.i.d.}}{\sim} \mathcal{N}(0, 0.5^2)$  for  $t \leqslant \theta_1$  and  $t \geqslant \theta_2 + 1$ , and  $\varepsilon_t \stackrel{\text{i.i.d.}}{\sim} \text{Ex}(0.5) - 0.5 \text{ for } \theta_1 + 1 \leqslant t \leqslant \theta_2, \text{ with } q = 2 \text{ and } (\theta_1, \theta_2) = (333, 667).$

Additional simulations for differing sample sizes and simulations with uneven spacing between neighbouring segments examining the performance of the multiscale version of the multi-lag NP-MOJO procedure are given in the Supplementary Material. The above scenarios consider changes in the covariance of bivariate, non-Gaussian random vectors in (B5), changes in the autocorrelation (while the variance stays unchanged) in (C1), a change in the parameters of an arch(1, 1) process in (C3) and changes in higher moments of serially dependent observations in (D3). Table 1 reports the distribution of the estimated number of changepoints and the average covering metric (CM) and V-measure (VM) over 1000 realizations. Taking values between [0, 1], CM and VM close to 1 indicates better accuracy in changepoint location estimation; see the Supplementary Material for their definitions and complete discussions of the changepoint scenarios.

In the case of (C1), we have  $q_{\ell} = 0$ ,  $\ell \neq 1$ , while  $q_1 = 2$ , and thus we report  $\hat{q}_{\ell} - q_{\ell}$ for the respective single-lag NP-MOJO- $\ell$  procedure. Across all scenarios, the NP-MOJO- $\mathcal L$ procedure shows good detection and estimation accuracy and demonstrates the efficacy of considering multiple lags; see (C3) and (D3) in particular. As the competitors are calibrated for the independent setting, they tend to either over- or under-detect the number of changepoints in the presence of serial dependence in (C1), (C3) and (D3). In the Supplementary Material we compare the NP-MOJO procedure against changepoint methods proposed for time series data where it performs comparably to methods specifically calibrated for the changepoint scenarios considered.

Table 1. Distribution of the estimated number of changepoints and the average CM and VM over 1000 realizations. The modal value of  $\hat{q}-q$  in each row is given in bold, and the best performance for each metric is underlined for each scenario

				$\hat{q}$	$-q/\hat{q}_{\ell}-q$	<b>!</b> ℓ		
Model	Method	$\leq -2$	-1	0	1	$\geqslant 2$	CM	VM
(B5)	NP-MOJO-0	0.000	0.001	0.997	0.002	0.000	0.974	0.959
	NP-MOJO-1	0.005	0.121	0.867	0.007	0.000	0.931	0.927
	NP-MOJO-2	0.006	0.103	0.884	0.007	0.000	0.935	0.929
	NP-MOJO- $\mathcal{L}$	0.000	0.001	0.999	0.000	0.000	0.973	0.958
	E-divisive	0.670	0.189	0.101	0.032	0.008	0.431	0.335
	KCPA	0.322	0.000	0.662	0.015	0.001	0.775	0.725
(C1)	NP-MOJO-0	_	_	0.851	0.140	0.009	_	_
	NP-MOJO-1	0.000	0.002	0.956	0.042	0.000	0.978	0.961
	NP-MOJO-2	_	_	0.836	0.149	0.015	=	_
	$NP-MOJO-\mathcal{L}$	0.000	0.002	<u>0.986</u>	0.012	0.000	0.980	0.963
	E-divisive	0.001	0.001	0.012	0.035	0.951	0.685	0.686
	KCPA	0.792	0.002	0.065	0.025	0.116	0.399	0.132
	NWBS	0.013	0.001	0.007	0.015	0.964	0.398	0.558
	cpt.np	0.000	0.000	0.002	0.003	0.995	0.593	0.647
(C3)	NP-MOJO-0	_	0.409	0.533	0.056	0.002	0.744	0.484
	NP-MOJO-1	_	0.236	0.682	0.081	0.001	0.819	0.633
	NP-MOJO-2	_	0.299	0.626	0.073	0.002	0.787	0.571
	$NP-MOJO-\mathcal{L}$	_	0.210	0.727	0.062	0.001	0.823	<u>0.645</u>
	E-divisive	_	0.032	0.327	0.211	0.430	0.742	0.602
	KCPA	_	0.418	0.262	0.171	0.149	0.667	0.370
	NWBS	_	0.895	0.048	0.020	0.037	0.525	0.069
	cpt.np	_	0.000	0.013	0.047	0.940	0.634	0.554
(D3)	NP-MOJO-0	0.003	0.139	0.809	0.049	0.000	0.899	0.872
	NP-MOJO-1	0.006	0.155	0.792	0.047	0.000	0.892	0.864
	NP-MOJO-2	0.021	0.248	0.685	0.045	0.001	0.848	0.819
	NP-MOJO- $\mathcal{L}$	0.002	0.082	<u>0.914</u>	0.002	0.000	0.917	0.884
	E-divisive	0.005	0.002	0.072	0.118	0.803	0.681	0.707
	KCPA	0.441	0.012	0.481	0.052	0.014	0.667	0.500
	NWBS	0.047	0.015	0.139	0.124	0.675	0.680	0.676
	cpt.np	0.000	0.000	0.045	0.055	0.900	0.726	0.756

# 6. Data applications

# 6.1. California seismology measurement dataset

We analyse a dataset from the High Resolution Seismic Network, operated by the Berkeley Seismological Laboratory. Ground motion sensor measurements were recorded in three mutually perpendicular directions at 13 stations near Parkfield, California, USA for 740 s from 2 am on 23 December 2004. The data have previously been analysed by Xie et al. (2019) and Chen et al. (2022). Chen et al. (2022) pre-processed the data by removing a linear trend and down-sampling; the processed data are available in the ocdR package (Chen et al., 2020). According to the Northern California Earthquake Catalog, an earthquake of magnitude 1:47 Md hit near Atascadero, California (50 km away from Parkfield) at 02:09:54.01.

We analyse time series of dimension p=39 and length n=2000 by taking a portion of the dataset between 544 and 672 s after 2 am, which covers the time at which the earthquake occurred (594 s after). We apply the multi-lag NP-MOJO procedure with tuning parameters selected as in §4, using G=333 and the set of lags  $\mathcal{L}=\{0,...,4\}$ . We detect two changes at

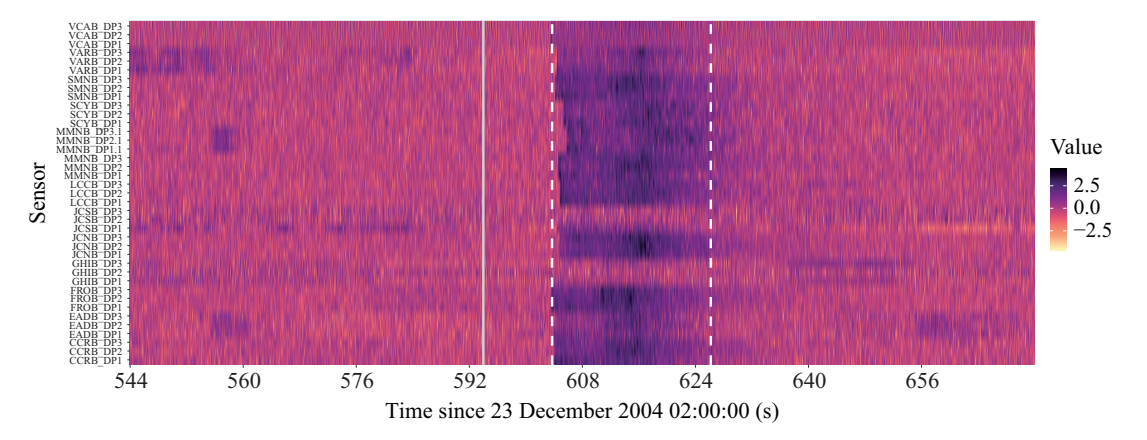


Fig. 3. Heat map of standardized sensor data. Changepoints detected by the multi-lag NP-MOJO procedure are shown with vertical dashed lines, and the time of the earthquake is represented by the solid vertical line.

all lags; the first occurs at between 603.712 and 603.968 s after 2 am and may be attributed to the earthquake. As noted by Chen et al. (2022), P waves, which are the primary preliminary wave and arrive first after an earthquake, travel at up to 6 km/s in the Earth's crust. This is consistent with the delay of approximately 9 s between the occurrence of the earthquake and the first changepoint detected by the multi-lag NP-MOJO procedure. We also note that performing online changepoint analysis, Xie et al. (2019) and Chen et al. (2022) reported a change at 603.584 and 603.84 s after the earthquake, respectively. The second change is detected at between 626.176 and 626.496 s after 2 am. It may correspond to the ending of the effect of the earthquake, as sensors return to baseline behaviour. Figure 3 plots the heat map of the data with each series standardized for ease of visualization, along with the onset of the earthquake and the two changepoints detected by the multi-lag NP-MOJO procedure. It suggests, amongst other possible distributional changes, that the time series undergoes mean shifts, as found by Chen et al. (2022). We also examine the sample correlations computed on each of the three segments; see Fig. 4 where the data exhibit a greater degree of correlation in segment 2 compared to the other two segments. Recalling that each station is equipped with three sensors, we note that pairwise correlations from the sensors located at the same stations undergo greater changes in correlations. A similar observation is made about the sensors located at nearby stations.

# 6.2. US recession data

We analyse the US recession indicator dataset. Recorded quarterly between 1855 and 2021 (n=667),  $X_t$  is recorded as a 1 if any month in the quarter is in a recession (as identified by the Business Cycle Dating Committee of the National Bureau of Economic Research), and 0 otherwise. The data have previously been examined for changepoints under piecewise stationary autoregressive models for integer-valued time series by Hudecová (2013) and Diop & Kengne (2021). We apply the multi-lag NP-MOJO procedure with G=111 and  $\mathcal{L}=\{0,\ldots,4\}$ . All tuning parameters are set as recommended in § 4 with one exception,  $\delta$  for kernel  $h_2$ . We select  $\delta=1$  for lag 0 and 2 otherwise, since pairwise distances for binary data are either 0 or 1 when  $\ell=0$  such that the median heuristic would not work as desired.

At all lags, we detect a single changepoint located between 1933:Q1 and 1938:Q2. The multi-lag NP-MOJO procedure estimates the changepoint at 1933:Q1, which is comparable to the previous analyses: Hudecová (2013) reported a change at 1933:Q1 and Diop &

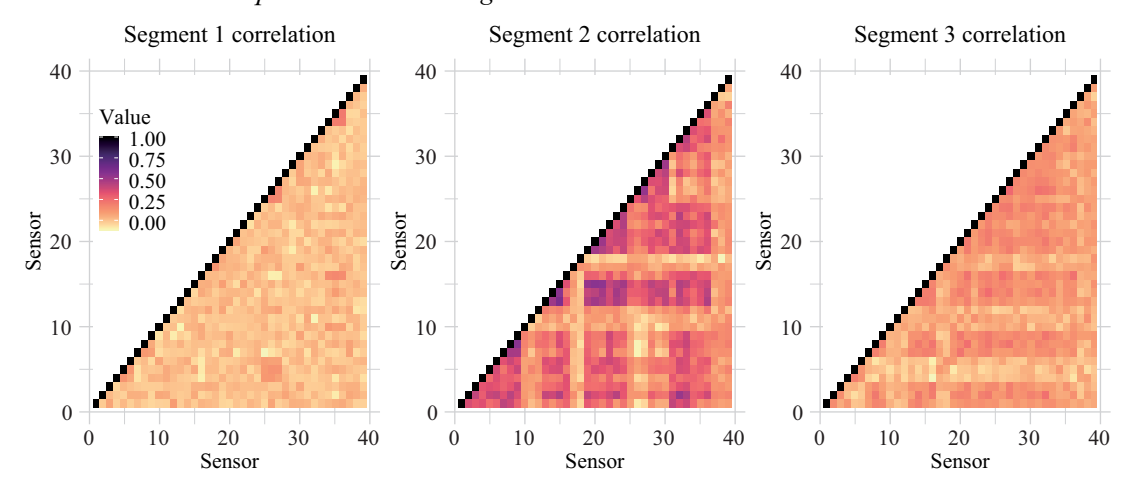


Fig. 4. Sample correlations from the three segments defined by the changepoint estimators.

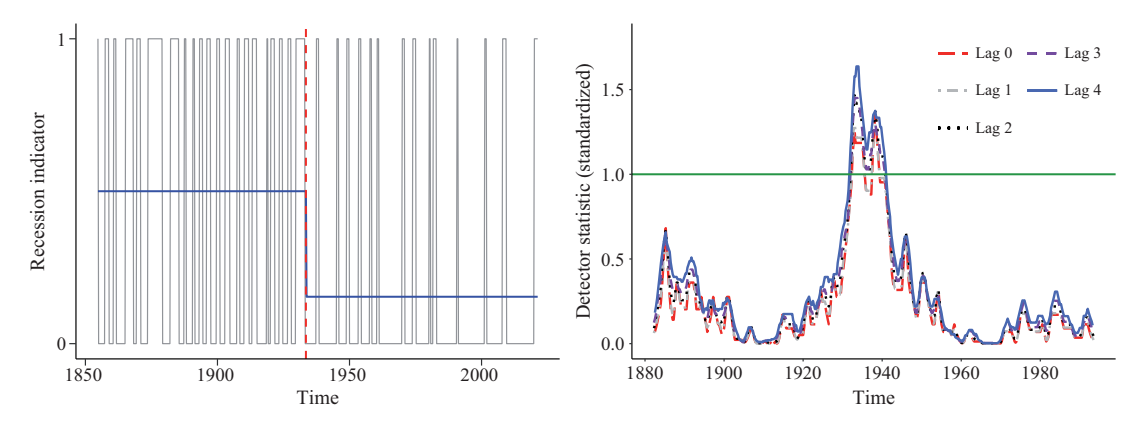


Fig. 5. (a) Quarterly US recession indicator series. A changepoint detected by the multi-lag NP-MOJO procedure is shown with a vertical dashed line and the sample means over the two segments with solid lines. (b) Plot of  $T_{\ell}(G,k)$ ,  $G \leq k \leq n-G$ , for lags  $\ell \in \mathcal{L}$ , after standardization by respective thresholds.

Kengne (2021) at 1932:Q4. The change coincides with the ending of the Great Depression and the beginning of World War II. Figure 5(a) plots the detected change along with the sample average of  $X_t$  over the two segments (superimposed on  $\{X_t\}_{t=1}^n$ ), showing that the frequency of recession is substantially lower after the change. Figure 5(b) plots the detector statistics  $T_{\ell}(G, k)$  at lags  $\ell \in \mathcal{L}$ , divided by the respective threshold  $\zeta_{\ell}(n, G)$  obtained from the bootstrap procedure. The thus standardized  $T_4(G, k)$ , shown with a solid line, displays the changepoint with the most clarity, attaining the largest value over the widest interval above the threshold (standardized to be one). At lag 4, the detector statistic has the interpretation of measuring any discrepancy in the joint distribution of the recession indicator series and its yearly lagged values.

#### ACKNOWLEDGEMENT

Work on this article was also carried out whilst McGonigle was affiliated with the School of Mathematics, University of Bristol. Cho is grateful to the support of the Leverhulme Trust via the Research Project Grant RPG-2019-390.

## E. T. McGonigle and H. Cho

### SUPPLEMENTARY MATERIAL

Supplementary Material contains additional discussion on the implementation of the NP-MOJO and multi-lag NP-MOJO procedures, the complete simulation results and the proofs of all theoretical results.

#### REFERENCES

- ARLOT, S., CELISSE, A. & HARCHAOUI, Z. (2019). A kernel multiple change-point algorithm via model selection. J. Mach. Learn. Res. 20, 1–56.
- Aue, A., Hörmann, S., Horváth, L. & Reimherr, M. (2009). Break detection in the covariance structure of multivariate time series models. *Ann. Statist.* 37, 4046–87.
- BAI, J. & PERRON, P. (1998). Estimating and testing linear models with multiple structural changes. *Econometrica* **66**, 47–78.
- BONIECE, B. C., HORVÁTH, L. & JACOBS, P. M. (2023). Change point detection in high dimensional data with U-statistics. *TEST* 33, 1–53.
- Carlstein, E. (1988). Nonparametric change-point estimation. Ann. Statist. 16, 188–97.
- CARR, J. R., BELL, H., KILLICK, R. & HOLT, T. (2017). Exceptional retreat of Novaya Zemlya's marine-terminating outlet glaciers between 2000 and 2013. *Cryosphere* 11, 2149–74.
- Celisse, A., Marot, G., Pierre-Jean, M. & Rigaill, G. (2018). New efficient algorithms for multiple change-point detection with reproducing kernels. *Comp. Statist. Data Anal.* **128**, 200–20.
- Chakraborty, S. & Zhang, X. (2021). High-dimensional change-point detection using generalized homogeneity metrics. *arXiv*: 2105.08976v1.
- CHEN, H. & FRIEDMAN, J. H. (2017). A new graph-based two-sample test for multivariate and object data. *J. Am. Statist. Assoc.* **112**, 397–409.
- CHEN, H. & ZHANG, N. (2015). Graph-based change-point detection. Ann. Statist. 43, 139–76.
- Chen, Y., Wang, T. & Samworth, R. J. (2020). ocd: high-dimensional, multiscale online changepoint detection. R package version 1.1.
- CHEN, Y., WANG, T. & SAMWORTH, R. J. (2022). High-dimensional, multiscale online changepoint detection. J. R. Statist. Soc. B 84, 234-66.
- Cно, H. & Fryzlewicz, P. (2012). Multiscale and multilevel technique for consistent segmentation of non-stationary time series. *Statist. Sinica* 22, 207–29.
- CHO, H. & FRYZLEWICZ, P. (2023). Multiple change point detection under serial dependence: wild contrast maximisation and gappy Schwarz algorithm. *J. Time Ser. Anal.* **45**, 479–94.
- CHO, H. & KIRCH, C. (2022). Two-stage data segmentation permitting multiscale change points, heavy tails and dependence. *Ann. Inst. Statist. Math.* **74**, 653–84.
- CHo, H. & Kirch, C. (2024). Data segmentation algorithms: univariate mean change and beyond. *Economet. Statist.* **30**, 76–95.
- CHU, C.-S. J., HORNIK, K. & KAUN, C.-M. (1995). MOSUM tests for parameter constancy. *Biometrika* 82, 603–17.
- Chu, L. & Chen, H. (2019). Asymptotic distribution-free change-point detection for multivariate and non-Euclidean data. *Ann. Statist.* **47**, 382–414.
- DAVIS, R. A., MATSUI, M., MIKOSCH, T. & WAN, P. (2018). Applications of distance correlation to time series. *Bernoulli* 24, 3087–116.
- DETTE, H., ECKLE, T. & VETTER, M. (2020). Multiscale change point detection for dependent data. *Scand. J. Statist.* 47, 1243–74.
- DIOP, M. L. & KENGNE, W. (2021). Piecewise autoregression for general integer-valued time series. *J. Statist. Plan. Infer.* **211**, 271–86.
- EICHINGER, B. & KIRCH, C. (2018). A MOSUM procedure for the estimation of multiple random change points. *Bernoulli* **24**, 526–64.
- FAN, Y., DE MICHEAUX, P. L., PENEV, S. & SALOPEK, D. (2017). Multivariate nonparametric test of independence. J. Mult. Anal. 153, 189–210.
- FOKIANOS, K. & PITSILLOU, M. (2017). Consistent testing for pairwise dependence in time series. *Technometrics* **59**, 262–70.
- FRICK, K., MUNK, A. & SIELING, H. (2014). Multiscale change point inference. *J. R. Statist. Soc. B* **76**, 495–580. FRYZLEWICZ, P. (2014). Wild binary segmentation for multiple change-point detection. *Ann. Statist.* **42**, 2243–81.
- FRYZLEWICZ, P. & SUBBA RAO, S. (2014). Multiple-change-point detection for auto-regressive conditional heteroscedastic processes. *J. R. Statist. Soc. B* **76**, 903–24.
- Gretton, A., Borgwardt, K. M., Rasch, M. J., Schölkopf, B. & Smola, A. (2012). A kernel two-sample test. J. Mach. Learn. Res. 13, 723–73.

- HARCHAOUI, Z., VALLET, F., LUNG-YUT-FONG, A. & CAPPÉ, O. (2009). A regularized kernel-based approach to unsupervised audio segmentation. In *Proc. 2009 IEEE Conf. Acoust. Speech Sig. Proces.*, pp. 1665–8. Los Alamitos, CA: IEEE Computer Society.
- HAYNES, K., FEARNHEAD, P. & ECKLEY, I. A. (2017). A computationally efficient nonparametric approach for changepoint detection. *Statist. Comp.* 27, 1293–305.
- HUDECOVÁ, S. (2013). Structural changes in autoregressive models for binary time series. *J. Statist. Plan. Infer.* **143**, 1744–52.
- Huskova, M. & Slaby, A. (2001). Permutation tests for multiple changes. Kybernetika 37, 605–22.
- Jewell, S. W., Hocking, T. D., Fearnhead, P. & Witten, D. M. (2020). Fast nonconvex deconvolution of calcium imaging data. *Biostatistics* **21**, 709–26.
- KILLICK, R., FEARNHEAD, P. & ECKLEY, I. A. (2012). Optimal detection of changepoints with a linear computational cost. *J. Am. Statist. Assoc.* **107**, 1590–8.
- KIRCH, C. & RECKRUEHM, K. (2024). Data segmentation for time series based on a general moving sum approach. *Ann. Inst. Statist. Math.* **76**, 393–421.
- KORKAS, K. K. & FRYZLEWICZ, P. (2017). Multiple change-point detection for non-stationary time series using wild binary segmentation. *Statist. Sinica* 27, 287–311.
- LAVIELLE, M. & TEYSSIERE, G. (2007). Adaptive detection of multiple change-points in asset price volatility. In *Long Memory in Economics*, Ed. G. Teyssière and A. P. Kirman, pp. 129–56. Berlin: Springer.
- LEUCHT, A. & NEUMANN, M. H. (2013). Dependent wild bootstrap for degenerate U- and V-statistics. *J. Mult. Anal.* 117, 257–80.
- LI, S., XIE, Y., DAI, H. & SONG, L. (2019). Scan B-statistic for kernel change-point detection. Seq. Anal. 38, 503–44.
- MADRID PADILLA, C. M., Xu, H., WANG, D., MADRID PADILLA, O. H. & Yu, Y. (2023). Change point detection and inference in multivariate non-parametric models under mixing conditions. In *Proc. 37th Int. Conf. Neural Info. Proces. Syst.*, pp. 21081–134. Red Hook, NY: Curran Associates.
- MADRID PADILLA, O. H., Yu, Y., WANG, D. & RINALDO, A. (2021). Optimal nonparametric change point analysis. *Electron. J. Statist.* **15**, 1154–201.
- MADRID PADILLA, O. H., Yu, Y., WANG, D. & RINALDO, A. (2022). Optimal nonparametric multivariate change point detection and localization. *IEEE Trans. Info. Theory* **68**, 1922–44.
- MATTESON, D. S. & JAMES, N. A. (2014). A nonparametric approach for multiple change point analysis of multivariate data. *J. Am. Statist. Assoc.* **109**, 334–45.
- McGonigle, E. T. & Cho, H. (2023). CptNonPar: nonparametric change point detection for multivariate time series. R package version 0.1.2.
- MEIER, A., KIRCH, C. & CHO, H. (2021). mosum: a package for moving sums in change-point analysis. *J. Statist. Software* **97**, 1–42.
- Messer, M., Kirchner, M., Schiemann, J., Roeper, J., Neininger, R. & Schneider, G. (2014). A multiple filter test for the detection of rate changes in renewal processes with varying variance. *Ann. Appl. Statist.* 8, 2027–67.
- MOKKADEM, A. (1988). Mixing properties of ARMA processes. Stoch. Proces. Appl. 29, 309–15.
- PAGE, E. S. (1954). Continuous inspection schemes. Biometrika 41, 100-15.
- PREUß, P., PUCHSTEIN, R. & DETTE, H. (2015). Detection of multiple structural breaks in multivariate time series. J. Am. Statist. Assoc. 110, 654–68.
- R DEVELOPMENT CORE TEAM (2025). R: A Language and Environment for Statistical Computing. Vienna, Austria: R Foundation for Statistical Computing. ISBN 3-900051-07-0, http://www.R-project.org.
- RAMDAS, A., REDDI, S. J., PÓCZOS, B., SINGH, A. & WASSERMAN, L. (2015). On the decreasing power of kernel and distance based nonparametric hypothesis tests in high dimensions. In *Proc. 29th Conf. Artif. Intel.*, pp. 3571–7. Washington, DC: AAAI Press.
- SAFIKHANI, A. & SHOJAIE, A. (2022). Joint structural break detection and parameter estimation in high-dimensional nonstationary VAR models. *J. Am. Statist. Assoc.* 117, 251–64.
- SEJDINOVIC, D., SRIPERUMBUDUR, B., GRETTON, A. & FUKUMIZU, K. (2013). Equivalence of distance-based and RKHS-based statistics in hypothesis testing. *Ann. Statist.* **41**, 2263–91.
- SZÉKELY, G. J., RIZZO, M. L. & BAKIROV, N. K. (2007). Measuring and testing dependence by correlation of distances. *Ann. Statist.* **35**, 2769–94.
- Tecuapetla-Gómez, I. & Munk, A. (2017). Autocovariance estimation in regression with a discontinuous signal and *m*-dependent errors: a difference-based approach. *Scand. J. Statist.* **44**, 346–68.
- Truong, C., Oudre, L. & Vayatis, N. (2020). Selective review of offline change point detection methods. *Sig. Proces.* **167**, 107299.
- Vanegas, L. J., Behr, M. & Munk, A. (2022). Multiscale quantile segmentation. J. Am. Statist. Assoc. 117, 1384–97.
- Wang, D., Yu, Y. & Rinaldo, A. (2021). Optimal covariance change point localization in high dimensions. *Bernoulli* 27, 554–75.
- Wu, W. B. (2005). Nonlinear system theory: Another look at dependence. Proc. Nat. Acad. Sci. 102, 14150-4.

- XIE, L., XIE, Y. & MOUSTAKIDES, G. V. (2019). Asynchronous multi-sensor change-point detection for seismic tremors. In 2019 IEEE Int. Symp. Info. Theory (ISIT), pp. 787–91. Piscataway, NJ: IEEE Press.
- Xu, H., Wang, D., Zhao, Z. & Yu, Y. (2024). Change point inference in high-dimensional regression models under temporal dependence. *Ann. Statist.* **52**, 999–1026.
- Yousuf, K. & Feng, Y. (2022). Targeting predictors via partial distance correlation with applications to financial forecasting. *J. Bus. Econ. Statist.* **40**, 1007–19.
- ZHAO, Z., JIANG, F. & SHAO, X. (2022). Segmenting time series via self-normalisation. J. R. Statist. Soc. B 84, 1699–725.
- ZHOU, Z. (2012). Measuring nonlinear dependence in time-series, a distance correlation approach. *J. Time Ser. Anal.* **33**, 438–57.
- Zou, C., Yin, G., Feng, L. & Wang, Z. (2014). Nonparametric maximum likelihood approach to multiple change-point problems. *Ann. Statist.* **42**, 970–1002.

[Received on 12 May 2023. Editorial decision on 17 March 2025]